Mon. Not. R. astr. Soc. (1968) **138,** 213–227.

THE ABUNDANCES OF THE ELEMENTS IN THE SOLAR PHOTOSPHERE—III

SILICON

D. L. Lambert and B. Warner†*

(Received 1967 August 1)

Summary

The solar photospheric abundance of silicon is derived from application of theoretical oscillator strengths for transition arrays of the type $3pns$–$3pn'p$ in Si I and $4s$–$4p$ in Si II. The two stages of ionization are in agreement and lead to log N(Si) = 7·55 on the scale where log N(H) = 12·00.

We discuss the interpretation of the profiles of strong Si I lines and suggest a modification of the solar model atmosphere. The [Si I] line at 10991·41 Å is found to be only a minor contributor to a blend with a telluric line.

1. *Introduction*

In a recent review of abundances in the solar photosphere, Müller (1967) concluded that the abundance of silicon is ill-determined. Indeed, her abundance compilation contains two entries for silicon: log N(Si) = 7·70 and log N(Si) = 7·24 on the standard scale log N(H) = 12·00. This uncertainty results from uncertainties in the absolute scale for the Si I oscillator strengths. The former value is based on laboratory determinations of oscillator strengths, and the latter on Coulomb approximation radial integrals with LS-coupling line strengths. In the present paper, the opportunity is taken to redetermine the silicon abundance using the results of intermediate coupling calculations for the Si I spectrum (Warner 1967). It is demonstrated that the abundance can be determined with an uncertainty of less than about 0·10 dex. This determination is based on selected Si I lines, and two Si II lines. A forbidden Si I line is also discussed.

The techniques of abundance determination, the model solar atmosphere, and the principal sources of observational data were described in the first paper of this series (Lambert 1968). The model atmosphere given there was used in the present calculations with the exception that for the analysis of certain strong lines a variant of this atmosphere was constructed and adopted. Full details are given in Section 2.2.1.

In much of the discussion the silicon abundance (log N(Si) = 7·50) derived by Goldberg, Müller & Aller (1960) will be adopted as a reference point. A revised abundance will be given as a logarithmic difference, that is

$$[\mathrm{Si}] = \log N(\mathrm{Si}) - \log N_{\mathrm{GMA}}(\mathrm{Si}).$$

2. *The Si* I *spectrum*

The number of identified Si I lines in the solar spectrum now totals several hundred. A detailed description of the presence of Si I lines in the Fraunhofer

* Present address: Mount Wilson and Palomar Observatories, Pasadena, California.
† Present address: Department of Astronomy, University of Texas, Austin, Texas.

spectrum is in preparation. The following Section discusses the theoretical oscillator strengths employed in this paper and, in particular, it emphasizes the criteria adopted for the selection of lines considered suitable for an abundance determination.

2.1 *Oscillator strengths.* The oscillator strengths used in this paper were selected from extensive intermediate coupling calculations (with allowance for configuration interaction where necessary) made by one of us (Warner 1967). The transitions included here were chosen on the grounds of:

(i) absence of configuration interaction;

(ii) reliability of the dipole transition integrals.

The radial integrals were calculated by the Scaled Thomas–Fermi–Dirac (STFD) method (Warner 1968) and only those which show little sensitivity to the energy parameters (i.e. absence of strong cancellation in the contributions to the dipole integral) were accepted.

Several transition arrays of the type $3s^2 3pns$–$3s^2 3pn'p$ are acceptable on the above precepts, but only four are at wavelengths suitable for use in the abundance study. They are $4s$–$4p$, $4p$–$5s$, $4p$–$6s$ and $4p$–$7s$. Transition arrays of the type $3s^2 3pnp$–$3s^2 3pn'd$ and $3s^2 3pnd$–$3s^2 3pn'f$ are not considered owing to the occurrence of configuration interaction (in $3s^2 3pnd$) with the resulting probable decrease in accuracy of the theoretical f-values.

In addition to the theoretical f-values, experimental measurements by Schulz (1966) at Kiel were considered. These refer to the $4s$–$5p$ array (see Table V), for which the theoretical approach is unreliable owing to cancellation in the dipole integral. The absolute scale of Schulz's f-values is not finalized (an increase of 0·20 dex* over the 1966 scale was recently reported (Müller 1967)) so that in the final assessment no weight is given to the result from the $4s$–$5p$ array. A measurement for one line from this same array (^1P–^1D, $\log gf = -1{\cdot}24$) was given by Hey (1959), which is 0·09 dex larger than the value given by Schulz in 1966.

2.2 *The Si* I *spectrum*

2.2.1 *The transition array* $4s$–$4p$. The lines from the $4s$–$4p$ array which are present in the solar spectrum are listed in Table I. Two new solar identifications for intercombination lines are included.

The lines in this array range in equivalent width from very large ($W_\lambda = 628$ mÅ) through medium to weak (minimum $W_\lambda = 4$ mÅ). In the interpretation of the strongest lines a number of problems were encountered. These are discussed first but it must be stressed that the absence of a completely successful interpretation for the strongest lines does not detract from the accuracy of the abundance determination because the abundance is reliably established from the weak lines in this and other transition arrays.

The first problem to be discussed relates to the measurement of the equivalent width. The weak but extensive wings of strong lines make a substantial contribution to the total equivalent width of the line. The depth of the line in the wings may be written as

$$r(\Delta\lambda) = C/\Delta\lambda^2$$

where C is a constant. For such a profile, the contribution to the equivalent width

* ' dex ' is equivalent to ' in the ten-based logarithm '.

TABLE I

Si I *lines: the transition array* $4s$–$4p$

Multiplet	Δj	$\lambda_\odot$	χ	log gf	W_λ	log W_λ/λ +7	Remarks†
$^3P^o$–^3D	2–3	12031·56	4·95	+0·43	460	2·58	MMH457, Mo470
	2–2	12270·76		−0·43	233	2·28	Mo
	2–1	12395·90		−1·66	88	1·85	Mo
	1–2	11984·50	4·93	+0·19	350:	2·47	Mo
	1–1	12103·62		−0·40	268	2·34	Mo
	0–1	11991·63	4·92	−0·16	350:	2·46	Mo366, L340
$^3P^o$–^3P	2–2	10827·14	4·95	+0·22	628	2·76	deJN628, L611, MMH456
	2–1	10979·34		−0·64	230:	2·32	L
	1–2	10603·43	4·93	−0·39	345	2·51	deJN345, L340, MMH296
	1–1	10749·39		−0·28	388	2·56	deJN388, L363, MMH266
	1–0	10786·85		−0·39	340	2·50	deJN340, L335, MMH242
	0–1	10660·99	4·92	−0·34	350	2·52	deJN350, L345, MMH277
$^3P^o$–^3S	2–1	10585·14	4·95	−0·02	470:	2·65	L470, MMH377
	1–1	10371·29	4·93	−0·71	212	2·31	L212, MMH185
	0–1	10288·95	4·92	−1·48	91	1·95	L91, MMH76
$^3P^o$–^1D	2–2	9768·35	4·95	−2·40	28	1·46	L
$^3P^o$–^1S	1–0	8435·28	4·93	−3·13	4:	0·67	RRT
$^1P^o$–^1D	1–2	10869·57	5·08	+0·32	600:	2·74	L600, MMH554
$^1P^o$–^1P	1–1	15888·55	5·08	−0·03	593	2·57	Mo
$^1P^o$–^1S	1–0	9413·51	5·08	−0·41	230:	2·39	L
$^1P^o$–^3P	1–2	12196·70	5·08	−2·88	16	1·12	Mo*
	1–1	12390·22		−1·81	75	1·78	Mo*
$^1P^o$–^3S	1–1	11890·48	5·08	−2·19	61	1·71	L

Notes :

* Denotes a new identification.

: Denotes an uncertain measurement.

† This column gives the individual measurements of the equivalent width.

Sources:

MMH = McMath Hulbert quoted by GMA.
Mo = Mohler (1955).
L = Delbouille & Roland Atlas (1963).
RRT = Moore, Minnaert & Houtgast (1966).
deJN = de Jager & Neven (1967).

from the interval $\Delta\lambda_0 \leqslant \Delta\lambda < \infty$ is

$$\Delta W_\lambda = r(\Delta\lambda_0) \times 2\Delta\lambda_0$$

Line profile observations for the $4s^3P^o$–$4p^3P$ multiplet (de Jager & Neven 1967) provide an illustrative example. For λ 10749 the wings with $r(\Delta\lambda) \leqslant 2$ per cent contribute about 40 mÅ or about 10 per cent to the total equivalent width. This contribution, which would probably be omitted if the noise level were about 2

per cent, is equivalent to a 30 per cent (0·11 dex) contribution in the abundance. It will be noted that the equivalent width measurements for the $^3P^o$–^3P multiplet exhibit a marked disagreement between the de Jager & Neven measurements and those obtained at the McMath–Hulbert Observatory. Measurements obtained from the Delbouille & Roland (1963) Atlas tracings are in good agreement with the former values. Photographic measurements by Allen (1938), which do not appear in Table I, are in reasonable agreement with the McMath–Hulbert data. This disagreement is probably attributable to an underestimate of the contribution from the extreme wings resulting from a combination of a higher noise level and lower resolution than are available with the Jungfraujoch spectrometer used by de Jager & Neven and by Delbouille & Roland. The latter measurements are adopted where available.

The central cores of the strong lines are formed in those regions of the model atmosphere ($\log \tau_0 \lesssim -3{\cdot}0$) for which the adopted temperature distribution is especially ill-determined (see Lambert 1967). It should not be surprising to find that an adjustment to the model in these outer layers is indicated through a comparison of the predicted and observed line profiles. In the adopted model the temperature decreased throughout the photosphere to attain a minimum value of 4730°K at $\log \tau_0 = -2{\cdot}5$ and then increased outwards to a constant ' boundary ' temperature of 4900°K. The computed profiles on the assumption of local thermodynamic equilibrium reflect this temperature distribution. The cores of the strong lines are predicted to be flat over about $\pm 0{\cdot}1$ to $\pm 0{\cdot}2$ Å at a central depth of about 45 per cent (see Fig. 1). This prediction is not confirmed by the observations. For example, λ 10827, which is the strongest line in the multiplet $^3P^o$–^3P, has a central depth of 73 per cent which decreases to about 57 per cent at 0·1 Å from the line centre. Two possibilities for resolving this discrepancy might be considered: the retention of the adopted temperature distribution with the introduction of non-LTE conditions for line formation or, alternatively, it might be possible to revise the temperature distribution to seek agreement with the observed profiles whilst retaining the assumption of LTE and, of course, agreement with the observations of the continuous spectrum in the far infrared and the ultra-violet.

Holweger (1967) has constructed a model atmosphere which together with the assumptions of LTE appears to be consistent with line profile observations for all lines except very strong resonance lines. In this model the temperature decreases outwards from 4400°K at $\log \tau_0 = -4{\cdot}0$ to 4210°K at $\log \tau_0 = -5{\cdot}0$, and the boundary temperature of 3900°K is approached at $\log \tau_0 = -6{\cdot}5$. In view of the success of this model, the Holweger temperature distribution for $\log \tau_0 \lesssim -2{\cdot}3$ was fitted smoothly onto the previously adopted temperature distribution. Holweger's values for the microturbulence were also adopted instead of the previously used value of 1·8 km/s at all depths. A typical profile computed with the revised model is shown in Fig. 1. Although the core is deepened the agreement with the observed profile (after correction for the instrumental profile) cannot be considered as completely satisfactory. It is estimated that the temperature must be further reduced to about 4000°K at $\log \tau_0 = -3$. However, it is likely that with this further modification the model would not be consistent with observations of the continuous flux distribution in the far infrared and the ultraviolet. Although this discussion prompts certain doubts about the validity of the assumption of LTE, the remaining discrepancies are of an insufficient magnitude to necessitate a full exploration in this paper: for example, for a typical line the difference at the line core between the

predicted and observed profiles amounts to an equivalent width discrepancy of less than 5 per cent, or an abundance difference of less than 15 per cent.

A curve of growth analysis for the $^3P^o$–^3P multiplet indicates that the abundance is [Si] = +0·35, which is significantly greater than the mean value [Si] = +0·05 which is suggested by the weaker lines in the $4s$–$4p$ and other arrays. Since the theoretical f-values are unlikely to be in error by a factor of two, an alternative explanation is sought. A possible explanation is that the damping constant should be increased above the calculated value. At the depth of formation of the Si I

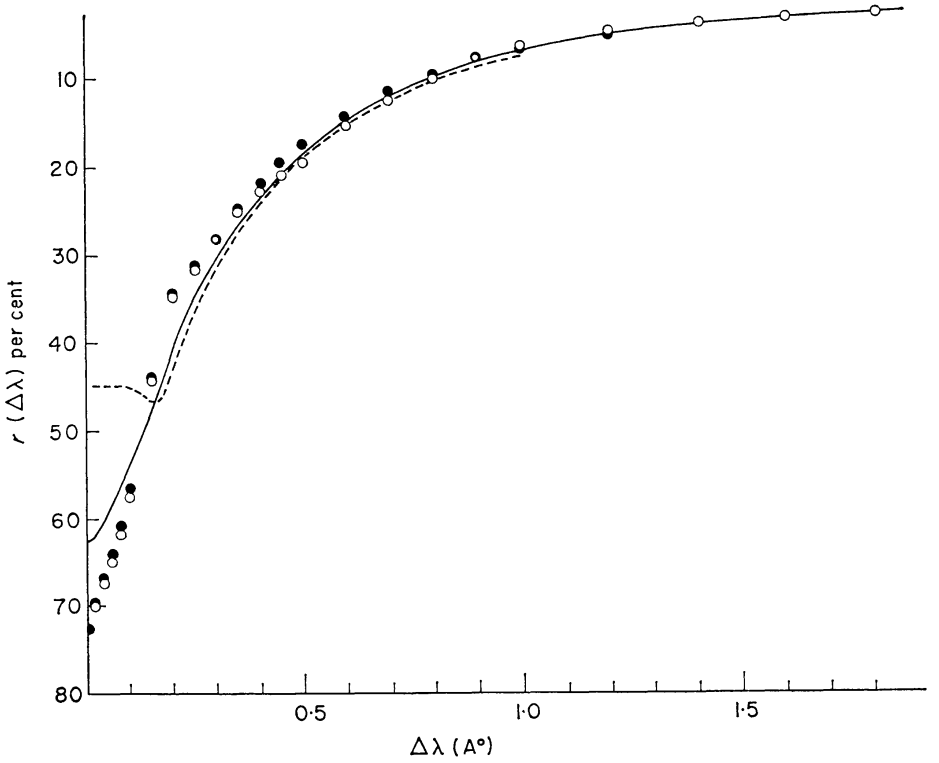

FIG. 1. *The line profile for* λ 10827 ($4s^3P_2^o$–$4p^3P_2$). *The observed profile (de Jager & Neven* 1967) *is shown by the filled circles (red wing) and the open circles (blue wing). The solid line shows the predicted profile for the modified model atmosphere. The broken line gives the predicted profile for the original model atmosphere with a boundary temperature of* 4900°K.

wings the principal contribution (greater than 80 per cent) to the damping is provided by Van der Waals broadening (this was calculated from the following mean square radii: $\overline{R_{up}^2}$ = 94·3 and $\overline{R_{low}^2}$ = 48·0 a.u.). The predicted and the observed profiles agree for [Si] = +0·05 when the damping constant is increased by a uniform factor $d = 2{\cdot}1 \pm 0{\cdot}2$. The predicted profiles with the increased damping constant must match the observations in the wings where the line depth is proportional to the product of the abundance and the damping constant. To within the uncertainties set by the present observations the profile also matches the observations in the core of the line. The derivation of the increased damping is dependent on the accuracy of the oscillator strengths but, as the f-values for the weak intercombination lines in this array provide a mean abundance (see below) in good agreement with results from other arrays, this supposition is probably correct. Unfortunately the reason for the increased damping is not yet apparent, but it

should be noted that similar deficiencies in the theoretical damping constants have been noted for the Na *D* lines (Chamaraux 1967; $d = 1{\cdot}8$ according to Lambert & Warner 1967), and in the O I λ 7774 triplet ($d = 2{\cdot}2$, Müller, Baschek & Holweger 1967).

The other lines in the $4s$–$4p$ array will be briefly discussed. For the multiplet $^3P^o$–^3D a curve of growth analysis with the modified model gives [Si] = −0·20. If the damping constant increase $d = 2{\cdot}1$ is applicable, the abundance is reduced to [Si] = −0·50, which is not consistent with the result from the weak Si I lines. The probable explanation is that the adopted equivalent widths (from Mohler (1955)) are in error. The solar spectra available to Mohler were probably similar or inferior with respect to noise and resolution to the McMath–Hulbert tracings which provided the equivalent widths for $^3P^o$–^3P. If it is assumed that a similar underestimate was made by Mohler, one obtains an abundance [Si] = 0·00 to 0·10 for $d = 2{\cdot}1$. Two lines λ 11984·50 and λ 11991·63 appear on the Delbouille & Roland Atlas but cannot be measured with sufficient precision to check the proposed explanation. Re-observation of this multiplet would be of interest.

The multiplet $^3P^o$–^3S gives the following results:

	Δj	2–1	1–1	1–0
$d = 1$		+0·37	+0·13	−0·15
	[Si]			
$d = 2{\cdot}1$		+0·10	−0·09	−0·21

As the equivalent widths for these lines are obtained from the Delbouille & Roland Atlas an appreciable systematic error is not expected. The principal feature of these results is the significant variation between lines. This variation is reduced but not eliminated when the damping constant is increased. As the adoption of LS coupling line strengths leads to a marked increase in the variation: [Si] = +0·60, −0·20, −0·74, one might suspect that the discrepancy will vanish with a subsequent refinement of the intermediate coupling calculations.

The multiplet $^1P^o$–^1D gives [Si] = 0·40 with $d = 1$. This result strongly suggests that the increase in damping constant to $d = 2{\cdot}1$ is applicable to this transition. $^1P^o$–^1P at λ 15888 gives [Si] = −0·17 with $d = 1$. No weight should be attached to this result in view of the probable underestimate of the equivalent width. The equivalent width of the remaining singlet $^1P^o$–^1S at λ 9413 is uncertain owing to possible blending with an atmospheric line, but with $d = 1$ the abundance [Si] = +0·24 is obtained.

The intercombination lines are substantially weaker and the interpretation is correspondingly simpler. The five lines in Table I give a mean abundance [Si] = +0·06, which is unchanged for $d = 2$. The mean abundance for all seven lines weaker than $\log W_\lambda/\lambda = -4{\cdot}80$ is [Si] = −0·01, or −0·03 with $d = 2$. The curve of growth is given in Fig. 2. The scatter suggests an uncertainty of at least ±0·05 dex.

2.2.2 *The transition array* $4p$–$5s$. Table II gives details of 12 lines from the $4p$–$5s$ array. One line is newly identified in the solar spectrum. The composite curve of growth is shown in Fig. 3. The mean abundance based on the 12 lines is [Si] = −0·05 with the standard theoretical damping constant ($d = 1$). With

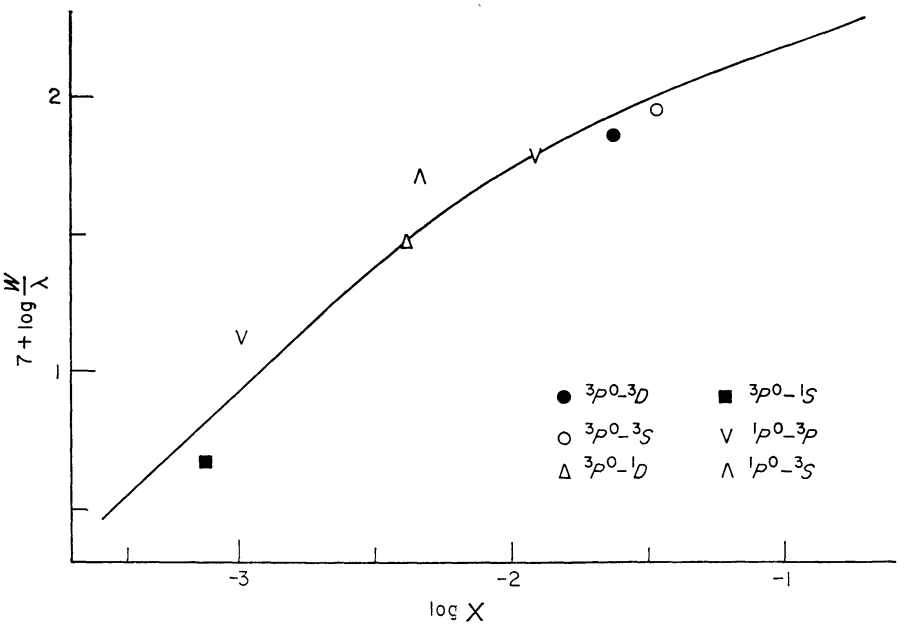

FIG. 2. *The curve of growth for the weaker lines* ($\log W_\lambda/\lambda \leqslant -4{\cdot}80$) *from the* $4s$–$4p$ *transition array. The solid line corresponds to* [*Si*] $= -0{\cdot}01$ *and* $d = 1$.

TABLE II

Si I *lines: the transition array* $4p$–$5s$

Multiplet	Δj	$\lambda_\odot$	χ	$\log gf$	W_λ	$\log W_\lambda/\lambda+7$	Remarks†
^3D–$^3P^o$	3–2	15960·17	5·98	+0·15	417	2·42	Mo
	2–2	15558·00	5·96	−0·72	180	2·06	Mo
	2–1	16094·96		−0·10	320	2·30	Mo
	1–2	15361·37	5·95	−1·95	23	1·18	Mo
	1–1	15884·48		−0·73	146	1·96	Mo
^3P–$^3P^o$	2–1	19505·86	6·10	−0·63	159	1·91	Mo
^3D–$^1P^o$	2–1	14769·88	5·96	−1·58	38	1·35	Mo
	1–1	14592·74	5·95	−1·42	89	1·79	Mo
^3P–$^1P^o$	1–1	17205·82	6·08	−1·55	44	1·41	Mo
^1D–$^1P^o$	2–1	21354·32	6·22	+0·09	388	2·26	Mo
^1P–$^1P^o$	1–1	13177·06	5·86	−0·49	250	2·28	Mo*
^1P–$^3P^o$	1–1	14221·52	5·86	−1·20	122	1·93	Mo

† See Notes to Table I.

increased damping constant ($d = 2{\cdot}1$) the mean abundance is decreased to [Si] $= -0{\cdot}16$.

It is shown below that the abundance [Si] $= +0{\cdot}05$ is suggested by the analysis of the weak lines in other arrays. The array $4p$–$5s$ would appear not to be in good agreement with this result. The probable explanation is that the equivalent widths from Mohler's (1955) catalogue are systematically in error. Unfortunately this

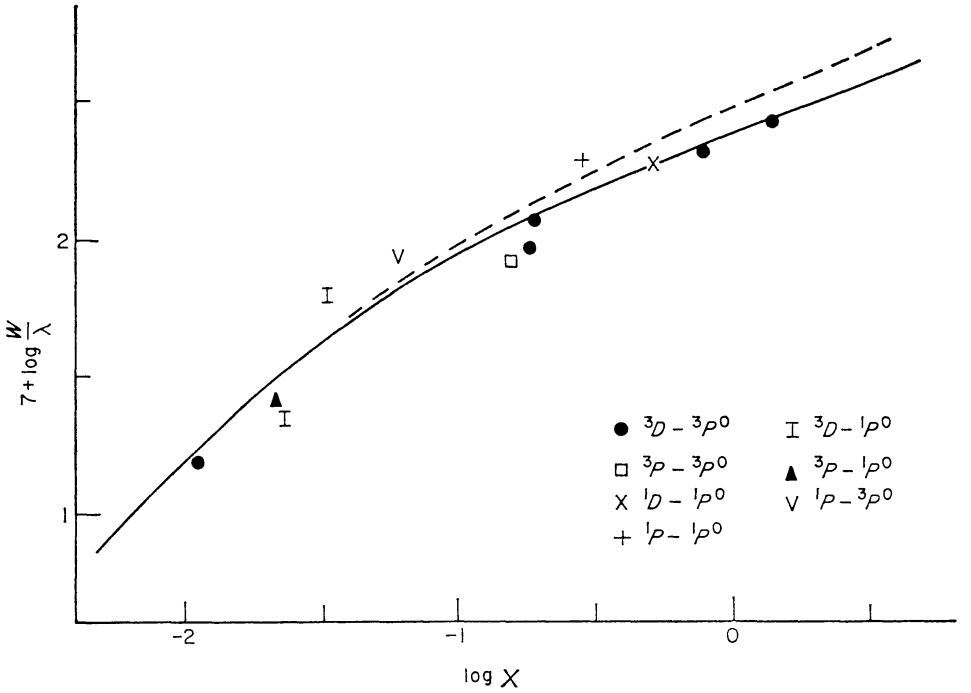

FIG. 3. *A composite curve of growth* ([*Si*] = −0·05) *for the* 4*p*–5*s transition array. The solid line gives the computed curve of growth for* λ 15850, χ = 5·96 *eV and d* = 1. *The broken line illustrates the effect of an increase in the damping constant to d* = 2. *The computed curves of growth for differing wavelengths were displaced to fit that for* λ 15850 *at log* W_λ/λ = −5·0.

TABLE III

Si I *lines: the transition array* 4*p*–6*s*

Multiplet	Δ*j*	$\lambda_\odot$	χ	log *gf*	W_λ	log W_λ/λ+7	Remarks†
^3D–$^3P^o$	3–2	8892·74	5·98	−0·83	77	1·94	L
	2–2	8766·42	5·96	−1·68	12	1·14	L12, RRT13
	2–1	8949·06		−1·12	48	1·73	L
	1–1	8883·68	5·95	−1·78	15	1·23	L
	1–0	8925·30		−1·42	32	1·56	L
^3P–$^3P^o$	2–2	9689·37	6·10	−1·09	49	1·70	L
	1–0	9839·36	6·08	−1·66	17	1·24	L
^3S–$^3P^o$	1–2	9891·61	6·13	−1·33	22	1·35	L
	1–1	10124·83		−2·10	6·0	0·77	L*
^3D–$^1P^o$	2–1	8667·37	5·96	−2·04	7·8	0·96	L7·8, RRT8
	1–1	8606·00	5·95	−2·14	7·8	0·95	L7·8, RRT9
^3P–$^1P^o$	0–1	9423·95	6·08	−2·65	2	0·33	L*
^1D–$^1P^o$	2–1	10582·16	6·22	−1·01	37	1·54	L
^1P–$^1P^o$	1–1	8093·23	5·86	−1·45	57	1·85	L54, RRT66
^1S–$^1P^o$	0–1	12458·50	6·40	−1·87	10	0·90	Mo*
^1D–$^3P^o$	2–1	11005·1	6·22	−1·98	3:	0·42	L*
^1P–$^3P^o$	1–1	8338·34	5·86	−1·90	17	1·32	L16, RRT19

† See Notes to Table I.

supposition cannot be checked owing to the lack of independent measurements of equivalent widths obtained from spectra with a resolution and noise level superior to that available to Mohler.

2.2.3 *The transition array* $4p$–$6s$. Seventeen lines from the $4p$–$6s$ array are listed in Table III. Four new solar identifications are included. The composite curve of growth is given in Fig. 4. The mean abundance is [Si] = +0·06, which is reduced by less than 0·01 dex if the damping constant is increased by a factor of 2.

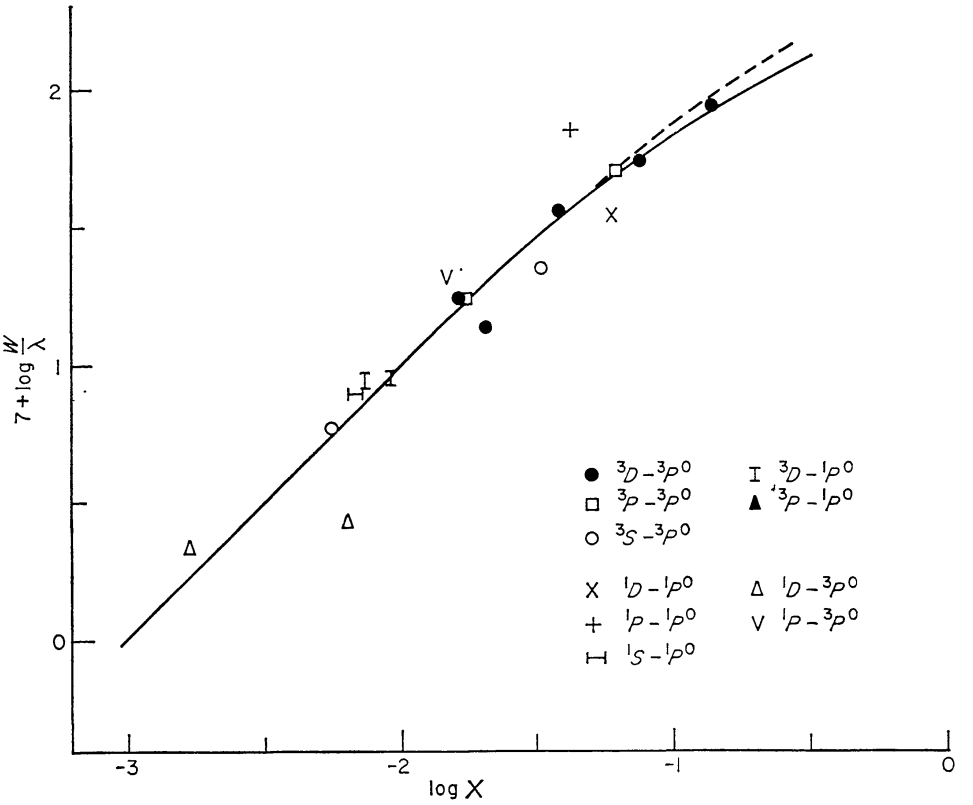

FIG. 4. *The curve of growth for the* $4p$–$6s$ *transition array. The solid line corresponds to* [*Si*] = +0·06. *The broken line illustrates the case* $d = 2$.

With the exception of two lines the scatter about the mean curve is probably attributable entirely to errors in the equivalent widths. The two exceptions are ^1P–$^1P^o$ with [Si] = +0·47 and ^1D–$^3P^o$ with [Si] = −0·33. The former also gives a significantly larger abundance in both $4p$–$5s$ and $4p$–$7s$. The mean abundance from the array is unchanged if these two lines are omitted.

2.2.4 *The transition array* $4p$–$7s$. Table IV gives the selected lines from the $4p$–$7s$ array. The composite curve of growth is shown in Fig. 5. The mean abundance from the 13 lines is [Si] = +0·10. If the four lines which differ from the mean by more than ±0·25 dex are omitted the mean is then [Si] = +0·11. The r.m.s. deviation for these nine lines is only ±0·04, which suggests that the scatter is produced by measurement errors in the equivalent widths.

2.2.5 *The transition array* $4s$–$5p$. It was pointed out in Section 2.1 that owing to cancellation in the transition integral the theoretical f-values are unreliable.

TABLE IV

Si I *lines: the transition array 4p–7s*

Multiplet	Δj	$\lambda_\odot$	χ	log gf	W_λ	log $W_\lambda/\lambda+7$	Remarks†
^3D–$^3P^o$	3–2	7373·01	5·98	−1·30	42	1·77	RRT
	2–2	7285·98	5·96	−2·15	5	0·84	RRT
	1–0	7395·54	5·95	−1·89	11	1·17	RRT
^3P–$^3P^o$	2–2	7912·38	6·10	−1·56	13	1·21	L13, RRT15
	2–1	8057·91		−2·21	1·3	0·21	L1·3, RRT2·5
	1–1	7975·58	6·08	−2·17	5·9	0·87	L5·9, RRT6
	1–0	8012·27		−2·13	5·0	0·80	L5·0, RRT10
^3S–$^3P^o$	1–2	8046·80	6·80	−1·80	6·5	0·89	L6·0, RRT7
^3D–$^1P^o$	2–1	7255·42	5·96	−2·33	4	0·74	RRT
^1D–$^1P^o$	2–1	8550·37	6·22	−2·33	8·2	0·98	L8·2, RRT9
^1P–$^1P^o$	1–1	6848·57	5·86	−2·08	15	1·34	RRT15, MMH16
^1D–$^3P^o$	2–1	8764·94	6·22	−2·22	5·5	0·80	L5·5, RRT2
^1P–$^3P^o$	1–1	6985·51	5·86	−2·34	2	0·45	RRT

† See Notes to Table I.

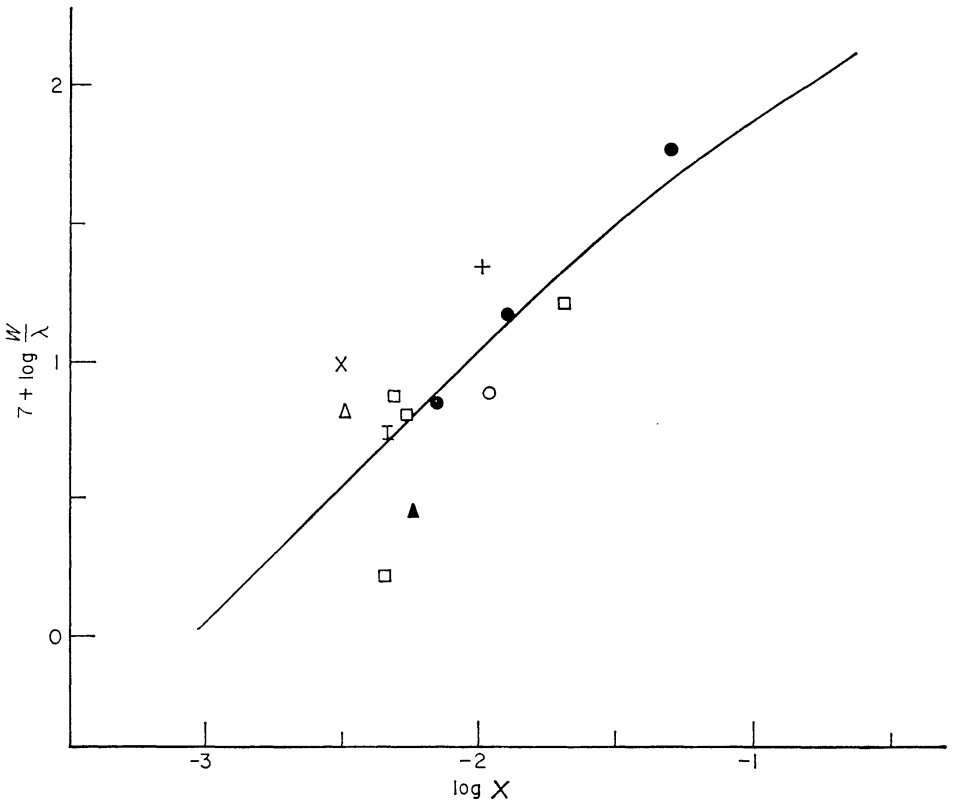

FIG. 5. *The curve of growth for the 4p–7s transition array. The solid line corresponds to* [*Si*] = +0·11. *The key to the symbols is given in Fig.* 4.

TABLE V

Si I *lines: the transition array* $4s$–$5p$

Multiplet	Δj	$\lambda_\odot$	χ	log gf*	W_λ	log $W_\lambda/\lambda+7$	Remarks†
$^3P^o$–^3D	2–3	5797·87	4·95	−2·07	38	1·82	RRT32, MMH44
	1–2	5793·08	4·93	−2·25	39	1·83	RRT38, MMH40
	0–1	5780·39	4·92	−2·55	24	1·62	RRT22, MMH27
$^3P^o$–^3P	2–2	5708·41	4·95	−1·63	77	2·13	RRT77, MMH77
	1–2	5645·62	4·93	−2·28	35	1·79	RRT35, MMH31
	1–1	5690·43		−2·06	53	1·97	RRT53, MMH52
	1–0	5701·11		−2·24	40	1·85	RRT40, MMH36
	0–1	5665·56		−2·23	40	1·85	RRT40, MMH38
$^1P^o$–^1D	1–2	5948·55	5·08	−1·33	88	2·18	RRT88, MMH89
$^1P^o$–^1S	1–0	5772·15	5·08	−1·95	46	1·89	RRT47, MMH45

* From Schulz (1966).

† See Notes to Table I, also MMH measurements include certain lines given by Holweger (1967).

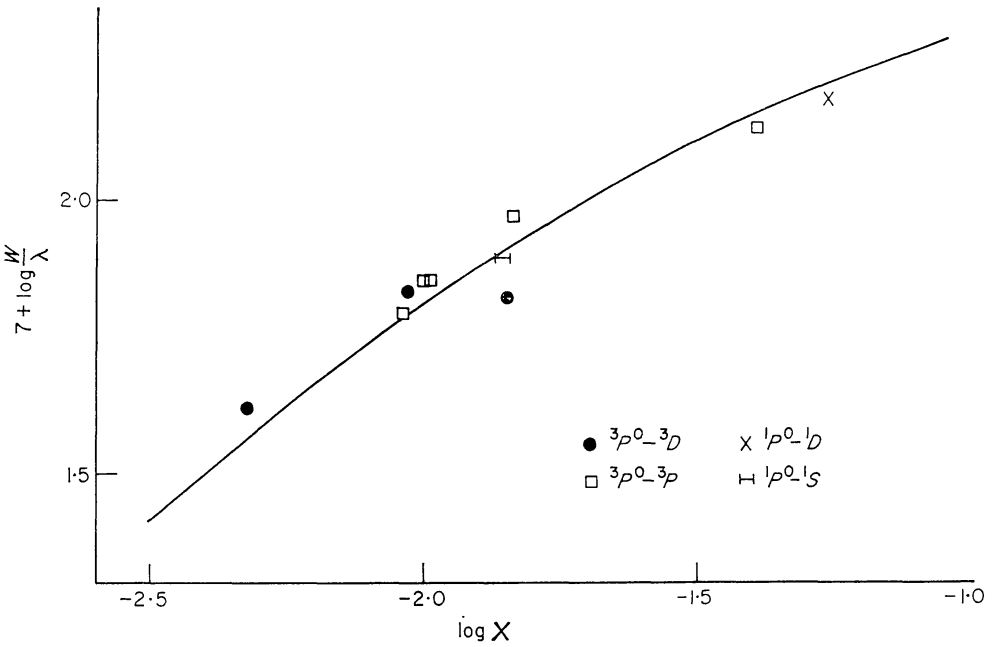

FIG. 6. *The curve of growth for the* $4s$–$5p$ *transition array drawn for* [*Si*] = +0·22 *and* d = 1.

Indeed, they lead to an abundance [Si] = −0·4 which is not consistent with the results from other arrays. Schulz (1966) measured the f-values for ten lines in the $4s$–$5p$ array. The curve of growth (Fig. 6), based on these f-values and the line list given in Table V, exhibits remarkably little scatter. However, the mean abundance [Si] = +0·22 (which is reduced by 0·05 dex for the case d = 2) is appreciably greater than is obtained from other arrays. Similar abundances based on different model atmospheres are reported by Grevesse (1967), Holweger (1967) and Müller (1967), whose results reduce to [Si] = +0·24, +0·17 and +0·20 respectively. This discrepancy suggests that the absolute scale for the experimental

f-values is in error. Müller (1967) reports that the 1966 scale should be increased by 0·20 dex. This would give [Si] = +0·02. Alternatively, one might consider normalization to the single measurement of Hey (1959). This (see Section 2.1) would give [Si] = +0·13. In view of the uncertainty over the absolute scale no weight will be attached to the abundance determinations from the $4s$–$5p$ array.

3. *The Si* II *spectrum*

3.1 *Introduction.* In the recent revision of Rowland's Preliminary Table (RRT), Moore, Minnaert & Houtgast (1966) list seven Si II lines, which are apparently present in the solar spectrum between λ 2935 and λ 8770. These seven lines and one other tentative identification (unidentified in RRT) are listed in Table VI. The proposed identifications and the possibility of their use for an abundance determination will be examined.

TABLE VI

Si II *lines in the solar spectrum*

Transition array	Multiplet	Δj	$\lambda_\odot$	χ	log gf	W_λ	log W_λ/λ +7	Remarks†
$3s3p^2$–$3s^24p$	^2D–$^2P^o$	5/2–3/2	3856·02	6·86	−0·66	45	2·07	RRT
		3/2–1/2	3862·60		−0·92	38	1·99	RRT
		3/2–3/2	3853·66		−1·62	23	1·78	RRT (1)
$3s^24s$–$3s^24p$	^2S–$^2P^o$	1/2–3/2	6347·10	8·12	+0·21	55	1·94	RRT54, MMH56
		1/2–1/2	6371·36		−0·09	31	1·69	RRT27, MMH34
$3s^23d$–$3s^24f$	^2D–$^2F^o$	5/2–7/2	4130·89	9·84	+0·77	26	1·80	RRT (2)
$3s^24p$–$3s^25s$	^2P–$^2S^o$	3/2–1/2	5978·93	10·07	−0·07	5·5	0·99	RRT (3)
		1/2–1/2	5957·56		−0·37	5·5	0·99	RRT (4)

Notes :

† See Notes to Table I.

(1) A CN line contributes to the measured equivalent width.

(2) This is a suspected blend according to the RRT.

(3) Identification given as Si II? in the RRT.

(4) Unidentified in the RRT.

3.2 *Oscillator strengths.* An inspection of the term diagram indicates that the combination of the Coulomb approximation radial integrals and LS coupling line strengths should provide reliable *f*-values in the majority of cases. Such values are listed in Table VI for all transitions except $3s3p^2$–$3s^24p$ for which LS coupling does not apply. Froese & Underhill (1966) computed Hartree–Fock wave functions allowing for configuration interaction. Their results are in good agreement with the Coulomb approximation calculations. Their results for $3s3p^2$–$3s^24p$ are adopted.

Experimental *f*-values are available for certain lines (Hey 1959, Schulz 1966). The experimental and theoretical results are compared in Table VII. The measurements by Hey are in good agreement with the theoretical results except for λ 5978. The measurements by Schulz for the multiplet $4s$–$4p$ are a factor two smaller than the theoretical results. Müller (1967) reported an increase of 0·20 dex in the absolute scale for the 1966 measurements of Si I lines but does not indicate whether a similar adjustment is applicable to the Si II data. Table VII suggests that the correction factor is common to the Si I and Si II data.

TABLE VII

log gf values for lines of the Si II spectrum

	log gf*			
λ	CA	FU	H	S
3856		−0·66	−0·74	
3862		−0·92	−0·97	
3853		−1·62		
6347	+0·21	+0·28		−0·03
6371	−0·09	−0·02	−0·05	−0·31
4130	+0·77	+0·76		
4128	+0·62	+0·58		
5978	−0·07	+0·02	−0·22	
5957	−0·37	−0·28		

* CA = Coulomb approximation.
FU = Froese & Underhill (1966).
H = Hey (1959).
S = Schulz (1966).

3.3 *Abundance analysis.* Curves of growth were calculated for the multiplets listed in Table VI, but only the $4s^2S$–$4p^2P^o$ is considered suitable for an abundance determination. The other multiplets are discussed in the following Section.

With Coulomb approximation *f*-values the following abundances are obtained from $4s^2S$–$4p^2P^o$:

$$\lambda\,6347 \quad [\mathrm{Si}] = +0{\cdot}15$$

$$\lambda\,6371 \quad [\mathrm{Si}] = -0{\cdot}06$$

and the mean abundance [Si] = +0·05 is consistent with results from the Si I lines.

3.4 *Discussion.* A straightforward analysis for the transition $3s3p^2$–$3s^24p$ gives [Si] = −0·31, which is significantly smaller than the above result (λ 3853·66 was not included owing to blending with a CN line). Inspection of the Utrecht Atlas reveals that both λ 3856 and λ 3862 are appreciably blended, with the latter barely discernible as a separate line. A large error in the abundance must be anticipated. The line λ 4130 suggests [Si] = +0·21 but according to the RRT the Fraunhofer line is probably a blend and no weight can be given to this result. Finally, both λ 5978 and λ 5957 give [Si] = +0·5, which may be supposed a sufficient reason to reject these tentative identifications.

4. *The [Si I] line:* $3p^2\,{}^1D_2$–$3p^2\,{}^1S_0$

The predicted wavelength for the forbidden transition ${}^1D_2$–${}^1S_0$ within the $3p^2$ ground configuration is 10 991·41 ± 0·01 Å from the improved energy levels for Si I given by Radziemski *et al.* (1967). Bowen (1948) first suggested that this line should be of a sufficient intensity to be detectable in the solar spectrum. Babcock & Moore (1947, p. 12) report the detection of this line but give no estimate for its equivalent width. The Delbouille and Roland Atlas (1963) shows that there is a line at the predicted wavelength with an equivalent width of about 8 mÅ. However,

Babcock & Moore list an atmospheric water vapour line at this wavelength (10 991·40 Å). It is likely, therefore, that the measured feature is a blend and not wholly attributable to the [Si I] line.

An estimate for the predicted intensity of the [Si I] line confirms this conclusion. The f-value was calculated using the methods of Pasternak (1940) and Garstang (1951). The electric quadrupole integral, as calculated by the Hartree–Fock and STFD methods, is only one-half that adopted by Pasternak and therefore the f-value is approximately one-quarter of his, that is $A_q = 0{\cdot}854\ s^{-1}$ or $gf = 1{\cdot}55 \times 10^{-8}$. Full details of the calculation are given elsewhere (Warner 1967).

With the revised abundance for Si the predicted equivalent width for the [Si I] line is 1·6 mÅ. The large discrepancy between the observed and predicted strength can be attributed to the identified atmospheric line.

From a careful analysis of spectra obtained at a high altitude station and over a range in zenith distance it should be possible to separate out the solar component to the blend at λ 10991·40. Furthermore, in observations of the west limb of the Sun the [Si I] line would be shifted by 0·06 Å into the red wing of the atmospheric line. Examination of the transition probabilities for other forbidden transitions indicates that no further [Si I] lines are expected to be present in the solar spectrum.

5. *Concluding remarks*

The abundance determinations from the Si I and Si II lines are summarised in Table VIII. Two points should be noted. Firstly, the results from four transition arrays in Si I are in good agreement: total spread with the increased damping is 0·27 dex but since the $4p$–$5s$ determination may be based on inaccurate equivalent widths, this spread could be as small as 0·14 dex. Secondly, the determination from the two Si II lines is in satisfactory agreement with the Si I results.

TABLE VIII

Summary of abundance results

Spectrum	Transition array	No. of lines	[Si] $d = 1$	[Si] $d = 2$
Si I	$4s$–$4p$	7	−0·01	−0·03
	$4p$–$5s$	12	−0·05	−0·16
	$4p$–$6s$	17	+0·06	+0·06
	$4p$–$7s$	9	+0·11	+0·11
Si II	$4s$–$4p$	2	+0·05	+0·02

The mean abundance with equal weight given to all lines is [Si] = +0·03 for $d = 1$ or 0·00 for $d = 2$. If the transition array $4p$–$5s$ is omitted the results are [Si] = +0·06 and +0·05 for $d = 1$ and $d = 2$ respectively. The result [Si] = +0·05 is adopted and the silicon abundance is

$$\log \frac{N(\mathrm{Si})}{N(\mathrm{H})} = -4{\cdot}45 = 7{\cdot}55 - 12{\cdot}00.$$

The uncertainty in this determination is less than ±0·10 dex and possibly as small as ±0·05 dex.

Silicon is one of two principal electron contributors in the outer layers of the photosphere (magnesium is the other). As the derived abundance is in good agreement with that adopted ($\log N(\mathrm{Si})/N(\mathrm{H}) = -4{\cdot}53$) for the calculation of the gas

and electron distribution, a recalculation using the revised abundance would lead to a negligible ($< 0{\cdot}005$ dex) revision of the above result.

Acknowledgment. During this work Warner has been supported by the Radcliffe–Henry Skynner Senior Research Fellowship at Balliol College, Oxford.

Department of Astrophysics,
Oxford.
1967 *August.*

References

Allen, C. W., 1938. *Astrophys. J.*, **88,** 125.
Babcock, H. D. & Moore, C. E., 1947. *The Solar Spectrum* λ 6600–λ 13495, Carnegie Institute, Washington.
Bowen, I. S., 1948. *Rev. mod. Phys.*, **20,** 109.
Chamaraux, P., 1967. *Ann Astrophys.*, **30**, 67.
Delbouille, L. & Roland, G., 1963. *Photometric Atlas of the Solar Spectrum from* λ 7498–λ 12016, Liège.
Froese, C. & Underhill, A. B., 1966. *Astrophys. J.*, **146,** 301.
Garstang, R. H., 1951. *Mon. Not. R. astr. Soc.*, **111,** 115.
Goldberg, L., Müller, E. A. & Aller, L. H., 1960. *Astrophys. J., Suppl. Ser.*, **5,** 1.
Grevesse, N., 1967. Report on Symposium No. 1. Assoc. Int. Geochim. Cosmochim., Paris, in press.
Hey, P., 1959. *Z. Phys.*, **157,** 79.
Holweger, H., 1967. *Z. Astrophys.*, **65,** 365.
de Jager, C. & Neven, L., 1967. *Bull. astr. Insts Neth. Suppl.*, **1,** 325.
Lambert, D. L., 1967. *Mon. Not. R. astr. Soc.*, **138,**143.
Lambert, D. L. & Warner, B., 1967. *Mon. Not. R. astr. Soc.*, **138,**181.
Moore, C. E., Minnaert, M. G. J. & Houtgast, J., 1966. *The Solar Spectrum* 2935–8770 Å, National Bureau of Standards, Monograph 61.
Müller, E. A., 1967. Report on Symposium No. 1. Assoc. Int. Geochim. Cosmochim., Paris, in press.
Müller, E. A., Baschek, B. & Holweger, H., 1967. *Solar Physics*, in press.
Pasternak, S., 1940. *Astrophys. J.*, **92,** 129.
Radziemski, L. J., Andrew, K. L., Kaufman, V. & Litzen, L., 1967. *J. opt. Soc. Am.*, **57,** 336.
Schulz, E., 1966. Thesis, Kiel University.
Warner, B., 1968. In preparation.